Available online at www.sciencedirect.com
SCIENCE DIRECT®
Separation and Purification Technology 42 (2005) 249–257
Separation Purification Technology
www.elsevier.com/locate/seppur

Microporous sol–gel derived aminosilicate membrane for enhanced carbon dioxide separation

George Xomeritakis[a], Chung-Yi Tsai[b,**], C. Jeffrey Brinker[a,c,*]

[a] *NSF Center for Micro-Engineered Materials, 203 Farris Engineering Center, The University of New Mexico, Albuquerque, NM 87131, USA*
[b] *United Technologies Research Center (UTRC), 411 Silver Lane, MS 129-90, East Hartford, CT 06108, USA*
[c] *Sandia National Laboratories, Advanced Materials Laboratory, 1001 University Blvd. SE, Suite 100, Albuquerque, NM 87106, USA*

Received 26 April 2004; received in revised form 20 August 2004; accepted 24 August 2004

Abstract

A new aminosilicate, sol–gel derived microporous inorganic membrane has been developed for enhanced CO_2 separation in applications such as removal of metabolic CO_2 from the breathing loop of the NASA extravehicular mobility unit (EMU), natural gas purification, or CO_2 capture from coal-fired power plant emissions. This membrane consists of an inorganic, amorphous silica matrix of pore size 4–5 Å, containing randomly dispersed amine ($-NH_2$) functional groups in order to enhance its CO_2 selectivity, due to preferential adsorption of CO_2 in the membrane pore walls and simultaneous blocking of permeation of other gases (O_2, N_2 and CH_4). It is found that the gas feed condition during permeation (partial pressure of CO_2, relative humidity), post-synthetic treatments and aging, affect significantly the separation performance of the membranes. At this stage of development, with feeds of 1–20 vol.% CO_2 and 0–40% relative humidity at 22 °C, the highest CO_2:N_2 separation factor was in the range 100–200, while the CO_2 permeance was in the range 0.1–1.5 cm^3 (STP)/(cm^2 min atm). The results suggest that controlling the membrane pore size and method of activation of amine groups are the most critical factors for improving the CO_2-permselectivity of the membrane.

Keywords: Silica membrane; Carbon dioxide separation; Sol–gel; Molecular sieving; Amine group

1. Introduction

Membrane-based separation of CO_2 from gas streams is an important unit operation and can find application in natural gas purification, CO_2 capture from emissions of coal-fired power plants, and in metabolic CO_2 removal from space life-supporting systems (extravehicular mobility unit (EMU), space shuttle or space station). With respect to the latter application, using space vacuum to remove metabolic CO_2 and H_2O vapor, membrane-based life-supporting systems have potential to reduce weight/volume/power requirements and minimize consumables, and therefore enable long-mission duration.

Separation of CO_2 with common polymeric or inorganic (e.g. zeolite, sol–gel silica or carbon molecular sieve) membranes, is achieved by differences in diffusion rates and/or adsorption strengths of mixture components in the polymer matrix or the inorganic membrane pores, and selectivity is usually rather low, e.g. 30–40 for CO_2:N_2 [1–5]. On the other hand, a number of recently developed immobilized liquid membranes (ILMs) exhibit high (>1000) CO_2:N_2 separation factors due to facilitated CO_2 transport mechanism [6–9], but their CO_2 permeation rate is rather low especially at moderate levels of relative humidity (RH) (<40%).

In order to overcome the inherent disadvantages of existing membranes, we have introduced the concept of a novel microporous aminosilicate membrane with fixed

* Corresponding author. Tel.: +1 505 272 7627; fax: +1 505 272 7336.
E-mail addresses: tsaica@utrc.utc.com (C.-Y. Tsai), cjbrink@sandia.gov (C.J. Brinker).
** Co-Corresponding author. Tel.: +1 860 610 7387; fax: +1 860 610 7911.

1383-5866/$ – see front matter © 2004 Elsevier B.V. All rights reserved.
doi:10.1016/j.seppur.2004.08.003

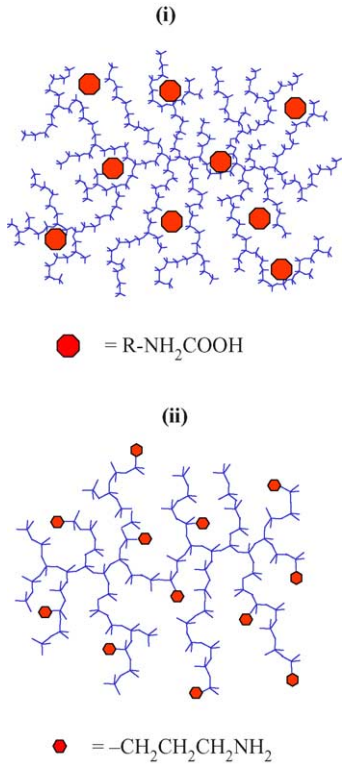

Fig. 1. Concept of a sol–gel derived, microporous aminosilicate membrane prepared using: (i) an amine salt, or (ii) an amine-containing alkoxysilane derivative as source of amine groups.

amine ligands incorporated in the silica matrix, in order to enhance membrane affinity for CO_2 separation [10]. With the combination of molecular sieving and selective adsorption/pore blocking transport mechanisms, the proposed membrane has potential to achieve high CO_2 separation performance, combined with enhanced structural stability. A schematic representation of this membrane is depicted in Fig. 1. The membrane consists of an inorganic microporous silica matrix prepared by a standard polymeric sol–gel route [5], which already exhibits high CO_2-permselectivity, e.g. CO_2:$CH_4 \sim 300$ and CO_2:$N_2 \sim 50$, due to the smaller kinetic diameter of CO_2 (3.3 Å) compared to that of N_2 (3.64 Å) or CH_4 (3.8 Å). In order to further enhance the CO_2 selectivity of the membrane, e.g. towards O_2, N_2 or CH_4, we have incorporated amine functional groups in the membrane matrix, in order to take advantage of the strong adsorption affinity of $-NH_2$ groups towards CO_2 in the presence of humidity.

The separation mechanism of this novel aminosilicate membrane is represented schematically in Fig. 2. For the case of an inert silica membrane (Fig. 2a), separation of CO_2 from O_2, N_2 or CH_4 is mainly based on differences in size of the gas molecules, and hence the separation factor is a strong function of the pore size of the membrane, which is difficult to control accurately [11,12]. On the other hand, when amine functional groups are randomly dispersed in the silica matrix (Fig. 2b), enhancement of CO_2 separation is possible, since CO_2 can adsorb strongly on the pore wall and reduce the effective pore diameter for permeation of non-adsorbing gases such as O_2, N_2 or CH_4.

A separation mechanism similar to that described in Fig. 2 has been reported for certain zeolite membranes and gas/vapor pairs, e.g. for *n*-butane:CH_4 with a MFI-type zeolite membrane [13], or for benzene:cyclohexane with a FAU-type zeolite membrane [14]. However, in these cases, there is no size selectivity of the particular membranes (e.g. ideal selectivities ~ 1), and the entire separation is based on stronger adsorption of one component in the membrane micropores and subsequent size exclusion of the weakly adsorbing component. On the other hand, the aim of the aminosilicate membrane depicted in Fig. 1 is to enhance the moderate size-based selectivity offered by the inert silica network itself (e.g. ~30–50 for CO_2:N_2), to a higher level as a result of additional adsorption effects in the membrane micropores.

It is pointed out here that other researchers proposed a similar approach for preparation of CO_2-permselective silica membranes, based on functionalizing the pore walls of mesoporous, surfactant-templated silica membranes with amine groups, in order to introduce affinity for CO_2 in the membrane [15]. However, due to the initial large pore size of these membranes (20–40 Å), we believe that it is quite difficult to achieve very high selectivities with this approach. Therefore, we have adopted a synthesis scheme based on incorporation of amine groups inside inert microporous silica membranes, prepared by an acid-catalyzed polymeric sol–gel route [5]. The aim of the present study is to explore the separation behavior of these newly developed aminosilicate microporous membranes using feed conditions that are relevant to EMU applications, although the membranes can be equally useful for other applications such as natural gas purification [1,5] or CO_2 capture/sequestration from coal-fired power plant emissions [16].

2. Experimental

2.1. Silica sol preparation

Our group has established a standard experimental protocol for synthesis of inert microporous silica membranes based on the following two-step procedure [5]. Firstly a mixture is prepared with molar composition (I), see Table 1. This mixture is reacted for 90 min at 60 °C under stirring, and the resulting 'stock sol' is stored in a −30 °C freezer for further use. For membrane deposition, additional H_2O and HCl are added to the stock sol, resulting in a 'standard sol' of composition (II), see Table 1. This mixture is aged for 24 h at 50 °C without agitation. After aging, two volumes of ethanol are added to one volume of the standard sol, to form a 'dipping sol' of final composition (III), see Table 1. After deposition and drying, the xerogel membrane is calcined for 3–6 h at 300 °C in vacuum, and can be further used for gas permeation experiments.

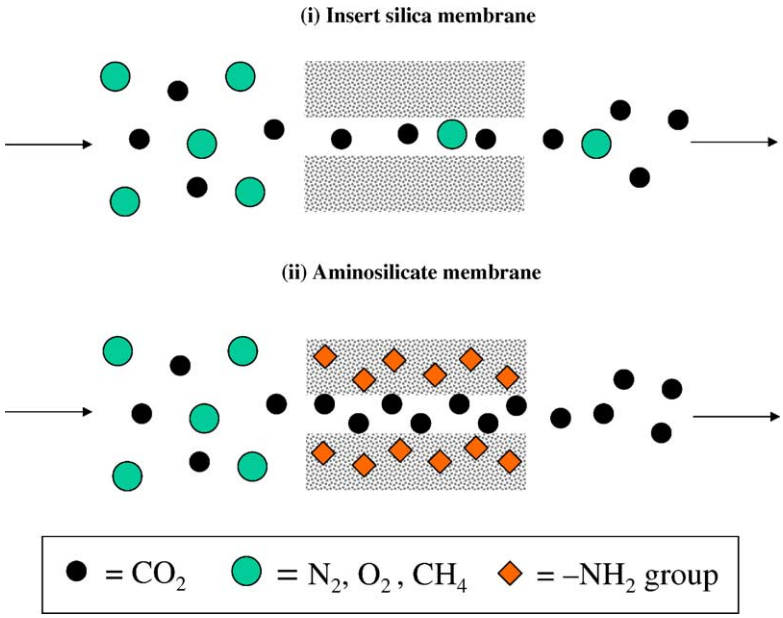

Fig. 2. Gas transport mechanism through: (i) a pure silica and (ii) an aminosilicate microporous molecular sieve membrane.

Incorporation of amine groups in our silica membranes was carried out by two different procedures. In the first procedure, which is based on an amine salt aqueous solution/silica sol mixing method, we employed sodium glycinate salt, CH_2NH_2COONa (GlyNa), as source of amine groups, since this water-soluble salt was used as active CO_2 carrier in an IML study reported recently [7]. In this case, the silica sol was prepared by adding suitable amounts of GlyNa, H_2O and HCl in stock sol (I), resulting in a clear sol of composition (IV), see Table 1. The molar ratio of $-NH_2$:Si was 0.1, 0.17, 0.25 and 0.33. It is noted that significant amounts of H_2O and HCl are necessary compared to sol (II), in order to avoid amine salt precipitation and silica sol gelation, respectively, due to the basic character of the amine groups. The clear glycine silicate sol is aged for 12, 24 or 48 h at 22 °C and is used for membrane deposition after dilution with proper amount of ethanol (final composition (V) in Table 1).

The second procedure is based on co-condensation of TEOS with an amine-containing alkoxysilane, here 3-aminopropyl triethoxysilane (APTES), with formula $(CH_3CH_2O)_3Si–CH_2CH_2CH_2NH_2$ [17,18]. In this case, the silica sol was a clear mixture of composition (VI), see Table 1 (molar ratio of $-NH_2$:Si = 0.2), which was aged for 24 h at 22 °C before membrane deposition. As with sol (IV), large amount of ethanol and HCl was necessary to avoid gelation of this sol, due to the basic character of $-NH_2$ groups in the APTES precursor. As seen in Fig. 1(b), the $-NH_2$ groups are covalently bonded to the silica matrix with this procedure, whereas the amine salt is physically trapped inside the silica matrix when the first preparation procedure is employed (Fig. 1a).

Table 1
Molar compositions of silica sols employed in previous [5] and present study, for microporous molecular sieve silica membrane preparation

Sol	Molar composition				
	Amine source[a]	TEOS	C_2H_5OH	H_2O	HCl
(I)	–	1.0	3.8	1.1	5.0×10^{-5}
(II)	–	1.0	3.8	5.0	4.0×10^{-3}
(III)	–	1.0	22.0	5.0	4.0×10^{-3}
(IV)	0.1–0.33	1.0	3.8	14.7	3.8×10^{-1}
(V)	0.1–0.33	1.0	22.0	14.7	3.8×10^{-1}
(VI)	0.2	0.8	22.0	5.0	4.0×10^{-1}

[a] Amine source is GlyNa for sols (IV) and (V), and APTES for sol (VI).

2.2. Membrane deposition

The support used for membrane deposition is a commercial asymmetric, multilayer ceramic alumina tube (Membralox, Pall Corp.), of length ~250 mm, o.d. 10 mm, i.d. 7 mm, and a final inner layer of 50-Å pore γ-Al_2O_3. This support is selected because of its good mechanical, chemical and thermal stability, smooth inner surface, and its convenient geometry for membrane deposition by dip coating. Before membrane deposition, the as-received support tube is cut in 55-mm long segments with a diamond wheel (Buehler), ultrasonicated in ethanol and calcined for 1 h at 400 °C in air. Subsequently, an intermediate sub-layer of surfactant-templated mesoporous silica (pore size 10–15 Å) is deposited in order to improve the finish of the γ-Al_2O_3 top layer [5,12], followed by calcination for 3 h at 450 °C in air. Deposition of the microporous aminosilicate membrane is carried out as described in detail in [5,12], using sols of composition (V) and (VI) in Table 1, followed by calcination for 3 h at 300–350 °C in vacuum (~1 Torr). Finally, the ends of the ceramic membrane tube are glazed with epoxy glue (Duraseal, Cotronics

Corp.) in order to repair any defects resulting from the diamond wheel-cutting step.

2.3. Membrane permeation

The permeation properties of the tubular aminosilicate membranes prepared as described above have been measured at 22 °C with the experimental set-up shown in Fig. 3. Sealing of the tubular ceramic membranes is achieved by compressing their glazed ends against elastomer gaskets, inside a custom-made stainless steel membrane holder [5,12]. Single-component permeation of a series of gases of increasing kinetic diameter is carried out by flowing a pressurized gas stream (100 cc/min, 15 psig) through the tubular membrane, and measuring the permeate flow rate exiting from the shell side of the permeation cell at ambient pressure with the aid of a calibrated soap-film flowmeter. The probe gases are He (2.6 Å), CO_2 (3.3 Å), Ar (3.4 Å), N_2 (3.64 Å), CH_4 (3.8 Å) and SF_6 (5.5 Å), in the order of increasing kinetic diameter. These measurements are useful for a rough estimate of the quality and pore size of the membranes, since gases with size smaller than the pore diameter would permeate through the membrane whereas larger molecules would be excluded.

The multicomponent gas separation properties of the membranes are determined by operating in the Wicke–Kallenbach counter-current flow configuration, with both the feed and permeate sides maintained at ambient pressure (e.g. no net pressure drop was applied across the membrane). The feed side is flushed by a ternary N_2–CO_2–$H_2O_{(v)}$ gas stream of variable composition (1–20 vol.% CO_2-balance N_2, 0–40% relative humidity), while the permeate side is flushed by a pure He stream, both at a total flow rate of 100 cc/min. Composition analysis of the permeate stream is carried out online with the aid of a HP 5890 Series II Gas Chromatograph equipped with a stainless steel packed column (Hayesep D, 100/120, Alltech) and thermal conductivity detector. N_2 is used to simulate air in the permeation experiments because of its similar physical properties with air and its chemical inertness, which allows for easier laboratory handling.

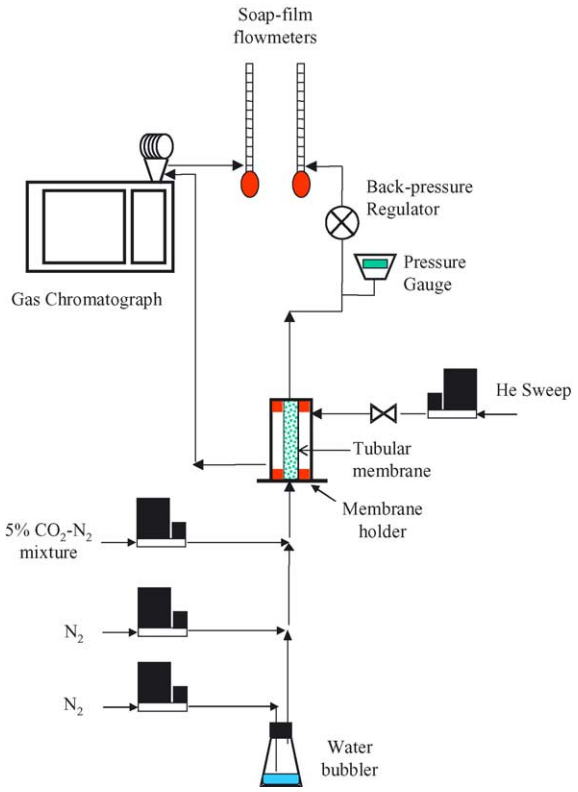

Fig. 3. Experimental set-up for single/multicomponent gas permeation.

3. Results and discussion

3.1. Membrane permeation

Fig. 4 shows representative single-component gas permeation results at 22 °C through an aminosilicate membrane sample prepared with APTES as amine source (ratio of $-NH_2$:Si = 0.2), as a function of kinetic diameter of the feed gases. Each feed gas was introduced at a pressure drop of $\Delta P = 1$ atm with respect to ambient, except for the case of SF_6 where a helium sweep was used to determine its very low permeance (Wicke–Kallenbach mode, $\Delta P = 0$ atm). The significant dependence of single-gas permeation on kinetic diameter of feed gas (e.g. ratio of He:SF_6 = 10,000), suggests that the membrane is microporous with average pore size <5 Å. Very similar experimental trends were also observed with membranes prepared with GlyNa as amine source. The pore size of the aminosilicate membranes prepared in this study must be slightly larger than the pore size of inert silica membranes reported recently (~3.5 Å, [5]), since the latter exhibited He:CH_4 selectivity of ~1500, as compared to only ~80 of the membrane shown in Fig. 4. This suggests that the $-NH_2$ groups incorporated in the silica matrix prevent complete interpenetration of the silica clusters contained in

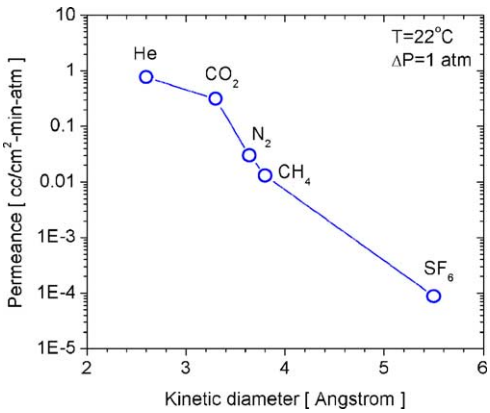

Fig. 4. Single-component gas permeation at 22 °C under a pressure drop of $\Delta P = 1$ atm, across a APTES:TEOS-derived aminosilicate membrane (ratio of $-NH_2$:Si = 0.2).

Table 2
Separation properties at 22 °C of different aminosilicate membrane samples with feeds of 1–2 vol.% CO_2-balance N_2

a/a	$-NH_2$ source	$-NH_2$:Si ratio	CO_2 in feed (%)	Relative humidity (%)	CO_2 permeance (cm^3 (STP)/cm^2 min atm)	Separation factor $\alpha(CO_2:N_2)$
1	GlyNa	0.17	2	2	1.39	52.3
2	GlyNa	0.1	2	2	0.33	62.6
3	GlyNa	0.1	2	2	1.03	60.1
4	GlyNa	0.17	2	2	0.29	100.0
5	GlyNa	0.25	2	0	0.97	77.3
6	APTES	0.2	2	2	0.23	41.0
7	APTES	0.2	2	5	0.53	49.9
8	APTES	0.2	1	0	0.38	70.2
9	APTES	0.2	1	20	0.14	76.8
10	APTES	0.5	1	40	0.32	52.9

Operation in the Wicke–Kallenbach mode under $\Delta P = 0$.

the silica sol during membrane deposition [19], and hence the average pore size of these membranes is slightly larger (e.g. 4–5 Å) compared to membranes prepared without amine groups.

Table 2 summarizes binary separation results obtained with humidified binary feeds of 1–2 vol.% CO_2-balance N_2 in the Wicke–Kallenbach mode, for different membrane samples prepared with GlyNa or APTES as amine source. As seen in Table 2, the binary CO_2:N_2 separation factors obtained from feeds of low CO_2 partial pressure lie in the range 40–100, and hence are significantly higher than respective ideal CO_2:N_2 selectivities (∼10, see Fig. 4), obtained with pressurized single-component feeds. This discrepancy suggests that the feed conditions (CO_2 partial pressure, relative humidity) have a significant effect on the apparent separation properties of the membrane, e.g. CO_2 permeance and/or $\alpha(CO_2:N_2)$, and further experiments were carried out in order to better understand the membrane permeation mechanism.

Fig. 5 shows the dependence of single-component CO_2 permeance on CO_2 feed partial pressure, obtained with dry feeds of 1–100 vol.% CO_2-balance He in the Wicke–Kallenbach operation mode, for an aminosilicate membrane sample prepared with APTES as amine source (ratio of $-NH_2$:Si = 0.2). As seen in the figure, the CO_2 permeance increases drastically as the CO_2 feed partial pressure is reduced down to 1–2 kPa, which suggests that adsorption effects may play important role during CO_2 permeation through the membrane. Indeed, when the partial pressure of CO_2 in the feed is rather low (1–2 kPa), the surface coverage of CO_2 in the membrane pore wall is small, and hence CO_2 can diffuse very fast through the membrane. However, when the CO_2 partial pressure in the feed is higher (≥0.5 atm), CO_2 coverage on the surface of the pore reaches a saturation level (Langmuir isotherm), resulting in slower CO_2 permeation due to effective reduction of the membrane pore size by the adsorbed CO_2 monolayer [20].

In order to further verify this hypothesis, we measured the transient behavior of CO_2 permeation through the same membrane sample, using a single-component CO_2 feed under a pressure drop of $\Delta P = 1$ atm across the membrane. As seen in Fig. 6, at the early stages of the experiment the permeance of CO_2 is quite high but then falls rapidly within the first 60 min and gradually stabilizes down to ∼20% of its initial level. In addition, the membrane could be regenerated, e.g. by flushing with helium, and the same permeation behavior was observed when CO_2 was fed again through the membrane. This result suggests that CO_2 permeation is quite fast during

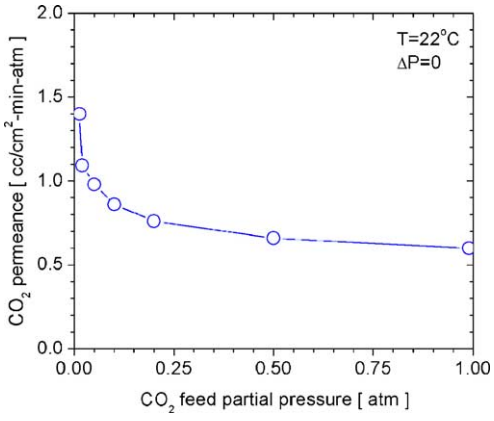

Fig. 5. Effect of CO_2 feed partial pressure on single-component CO_2 permeance for a APTES:TEOS-derived aminosilicate membrane (ratio of $-NH_2$:Si = 0.2). Feed is a binary CO_2:He mixture. Operation in the Wicke–Kallenbach mode under $\Delta P = 0$.

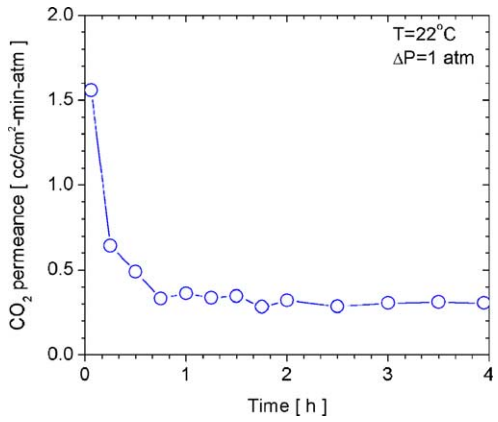

Fig. 6. Transient single-component CO_2 permeance under a pressure drop of $\Delta P = 1$ atm, for the same membrane sample shown in Fig. 5.

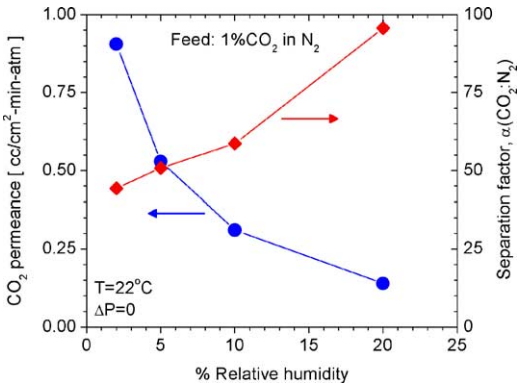

Fig. 7. Effect of relative humidity on CO_2 permeance and binary separation factor $\alpha(CO_2{:}N_2)$ for a APTES:TEOS-derived aminosilicate membrane (ratio of $-NH_2$:Si = 0.2). Feed is 1 vol.% CO_2-balance N_2. Operation in the Wicke–Kallenbach mode under $\Delta P = 0$.

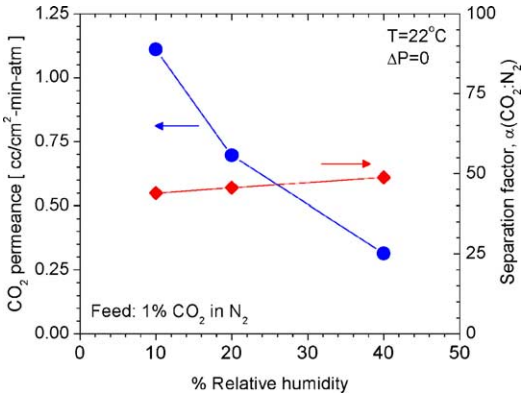

Fig. 8. Effect of relative humidity on CO_2 permeance and binary separation factor $\alpha(CO_2{:}N_2)$ for a APTES:TEOS-derived aminosilicate membrane (ratio of $-NH_2$:Si = 0.5). Feed is 1 vol.% CO_2-balance N_2. Operation in the Wicke–Kallenbach mode under $\Delta P = 0$.

the early states of permeation, since the surface coverage of the pore surface is low, but then progressive adsorption of CO_2 hinders the permeation due to effective reduction of the pore size of the membrane.

Other than CO_2, the partial pressure of H_2O vapor in the feed was also found to have significant effect on both the CO_2 permeance and $\alpha(CO_2{:}N_2)$ of the membrane. As seen in Fig. 7 for an APTES:TEOS-derived aminosilicate membrane (ratio of $-NH_2$:Si = 0.2), the CO_2 permeance from a 1 vol.% CO_2 feed decreases by a factor of six when the RH increases from 2 to 20%, while the $\alpha(CO_2{:}N_2)$ increases from ~40 to ~95, for the same increase in RH. Table 3 shows the effect of RH on the membrane permeation properties from a 50:50 (v/v) $CO_2{:}N_2$ feed, for the same membrane sample (#1). Again, similar trends are observed as with the 1 vol.% CO_2 feed case, shown in Fig. 7.

Fig. 8 shows the effect of RH on the permeation properties of another APTES:TEOS-derived aminosilicate membrane with higher amine loading (ratio of $-NH_2$:Si = 0.5). Because of the higher content of $-NH_2$ in this membrane, which may in turn affect its pore size and porosity [21], the CO_2 permeance at 20% RH was about six times higher than the respective sample in Fig. 7, but the $\alpha(CO_2{:}N_2)$ was less than 50. As seen in Table 3, an increase in RH from 0 to 50% has less effect on both the CO_2 permeance and $\alpha(CO_2{:}N_2)$, compared with the sample with lower amine loading.

Apart from the feed conditions, we observed that aging was another factor that influenced the permeation properties of our membranes. Fig. 9 shows the $CO_2{:}N_2$ separation property of the same membrane studied in Fig. 7, measured 2

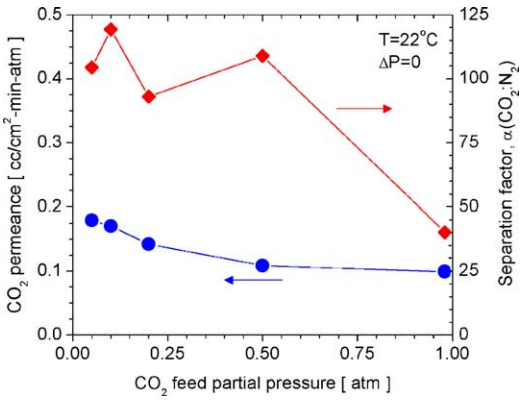

Fig. 9. Effect of CO_2 feed partial pressure on CO_2 permeance and binary separation factor $\alpha(CO_2{:}N_2)$ for a 2-month aged APTES:TEOS-derived aminosilicate membrane (ratio of $-NH_2$:Si = 0.2). Feed is a binary $CO_2{:}N_2$ mixture (RH = 0%). Operation in the Wicke–Kallenbach mode under $\Delta P = 0$.

months after its synthesis. With a CO_2 feed partial pressure of 0.05–0.5 atm (0% RH), the $\alpha(CO_2{:}N_2)$ of this membrane is ~100 (~40 right after synthesis), while the CO_2 permeance is now lower by a factor of four to five. Operation with moderate RH (5–10%) resulted in further decrease of the CO_2 permeance and increase of $\alpha(CO_2{:}N_2)$ to at least 150–200, which suggests that the separation factor could further increase at higher RH. However, operation at this condition was difficult since the sensitivity limit of the permeation apparatus was reached.

In order to explain the results in Fig. 9, we propose that aging results in further consolidation of the silica matrix and

Table 3
Effect of relative humidity on permeation properties at 22 °C of APTES:TEOS-derived aminosilicate membranes

Membrane	Ratio of $-NH_2$:Si	RH (%)	CO_2 permeance (cm^3 (STP)/cm^2 min atm)	Separation factor $\alpha(CO_2{:}N_2)$
#1	0.2	0	1.10	24.0
		50	0.09	88.8
#2	0.5	0	1.72	27.2
		50	0.46	43.6

Feed is 50:50 (v/v) binary $N_2{:}CO_2$ mixture. Operation in the Wicke–Kallenbach mode under $\Delta P = 0$.

hence decrease of the pore size, resulting in better size exclusion for N_2, but at the expense of CO_2 permeance. The presence of CO_2 in the feed results in an additional decrease of the N_2 permeance by a factor of 2.5, compared to its single-component value, since the ideal CO_2:N_2 selectivity is only 40 (right-most point in Fig. 9). Note that $\alpha(CO_2:N_2)$ is fairly independent for CO_2 feed partial pressure of 0.05–0.5 atm, which suggests that saturation of the membrane pores with CO_2 is achieved at lower CO_2 feed partial pressures for this aged membrane sample, as compared to a freshly-prepared sample, see Fig. 5.

3.2. Post-synthetic membrane treatment

A review of the gas separation results obtained with the new aminosilicate membranes developed in this study suggests that the $\alpha(CO_2:N_2)$ values lie in the range 50–90, and higher values, e.g. in the range of 100–200, can be obtained with aged samples, or samples exposed to humid atmosphere for prolonged time. The two most critical factors for obtaining better separation performance with our membranes are: (i) controlling the pore size of the membrane, and (ii) ensuring strong $–NH_2$:CO_2 interactions in the membrane pores during gas permeation. Regarding the membrane pore size, aging is one effective way to reduce it so that better size exclusion of N_2 is achieved but at the expense of membrane porosity, and hence permeance.

The activity of the amine groups incorporated in the silica matrix is also very important for achieving strong $–NH_2$:CO_2 interactions and effective blocking of N_2 permeation through the membrane. However, during aminosilicate sol preparation the amine groups have to be temporarily deactivated with HCl in order to prevent gelation of the sol, due to the basic nature of these groups, which will result in fast condensation of the silica clusters contained in the sol. The reaction of APTES with HCl can be represented as follows:

$$(OC_2H_5)_3Si–CH_2CH_2CH_2NH_2 + HCl \rightarrow (OC_2H_5)_3Si–CH_2CH_2CH_2NH_3^+Cl^-$$

Desorption of bound HCl from the amine groups after membrane deposition is essential for reactivation of the amine groups, and can be partially achieved during the vacuum calcination step (300–350 °C) following membrane deposition. Assuming that considerable amount of HCl still remains attached on the amine groups after membrane calcination, we examined the effect of various vapor treatments of the membrane, on CO_2 permeance and $\alpha(CO_2:N_2)$. As seen in Table 4, exposure of membranes to vapors of 1.0 N aqueous NH_4OH solution for 8–20 h resulted in reduction of both the permeance and selectivity of the membrane (membranes #1 and #2). This may probably be the result of formation of NH_4Cl salt in the membrane pores, and hence suggests that this treatment is not suitable for activation of the amine groups in the membrane. Membrane #3 was exposed to the vapors of a 10% ethanolamine, 10% H_2O, and 80% ethanol solution for 7 h (right after synthesis and before calcination), and showed reduced permeance but improved selectivity compared to samples #1 and #2.

Membrane #4 was flushed with a 100% RH N_2 stream while sealed in the permeation cell, while a dry N_2 stream was flushed through the permeate side in a counter-current mode. In this way, H_2O vapor permeated through the membrane during a 20-h treatment. Interestingly, with this water vapor stripping treatment, the membrane showed 50% improvement in selectivity with minor permeance loss after the treatment. Therefore, it is suggested that this step might aid in HCl desorption from the membrane microstructure, especially if it is carried out for longer times and at elevated temperatures (80–100 °C).

3.3. Comparison with pure silica membranes

Permeation measurements under the conditions described above were also carried out with pure silica membranes (with no amine groups) prepared as described in [5], using sol of composition (III) in Table 1, and some results are shown in Fig. 10. As seen in the figure, with a feed of 2 vol.% CO_2-balance N_2 and 0% RH, the membrane exhibits a CO_2 permeance of ~1.4 cm^3 (STP)/cm^2 min atm and $\alpha(CO_2:N_2)$ of ~26, consistent with previous reports [4,5]. Increasing the relative humidity in the feed up to 40% results in more than one order of magnitude decrease in the CO_2 permeance, with no substantial improvement for $\alpha(CO_2:N_2)$. Although the particular sample considered in Fig. 10 may not be entirely defect free as judged by its moderate $\alpha(CO_2:N_2)$, we still anticipate that the observed trends for CO_2 permeance and $\alpha(CO_2:N_2)$ are representative of the behavior of pure silica membranes, and specifically as regards the insensitivity of $\alpha(CO_2:N_2)$ in feed RH. This is indirect evidence that the presence of amine groups in the membranes prepared in this

Table 4
Effect of post-synthetic vapor treatments on permeation properties at 22 °C of membranes prepared with APTES as amine source (ratio of $–NH_2$:Si = 0.2)

Membrane	Treatment	Feed condition		CO_2 permeance (cm^3 (STP)/cm^2 min atm)		Separation factor $\alpha(CO_2:N_2)$	
		CO_2 (%)	RH (%)	Before	After	Before	After
#1	8 h NH_3 vapor	5	5	0.48	0.12	44.2	21.4
#2	20 h NH_3 vapor	10	10	0.28	0.016	64.5	30.6
#3	7 h $EtNH_2$ vapor	10	10	–	0.085	–	71.2
#4	20 h H_2O vapor	10	10	0.33	0.25	56.3	75.6

Operation in the Wicke–Kallenbach mode under $\Delta P = 0$.

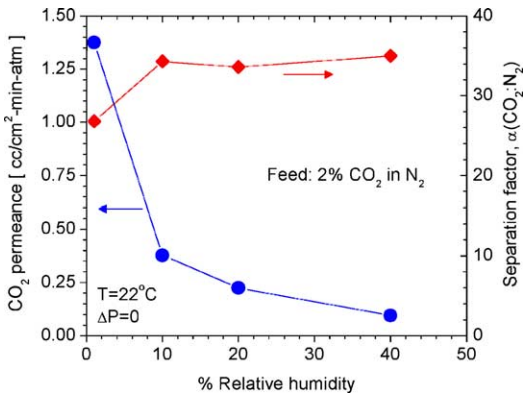

Fig. 10. Effect of relative humidity on CO_2 permeance and binary separation factor $\alpha(CO_2{:}N_2)$ for a TEOS-derived pure silica membrane. Feed is 2 vol.% CO_2-balance N_2. Operation in the Wicke–Kallenbach mode under $\Delta P = 0$.

study play important role in determining the separation properties of the membrane.

3.4. Comparison with other microporous inorganic membranes

Morooka and coworkers have reported in a number of publications [2,22-24] successful separation of equimolar $CO_2{:}N_2$ mixtures using ion-exchanged Y-type zeolite membranes grown on porous ceramic supports. Their most permeable membranes exhibit CO_2 permeance in the range 10–15 cm^3 (STP)/cm^2 min atm with $\alpha(CO_2{:}N_2)$ of ~40–50 (at 35 °C), while respective ideal selectivities are usually <10. However, the separation performance of these large-pore (~7 Å) zeolite membranes has not been studied with humidified feeds of lower CO_2 partial pressure (1–2 kPa) of interest here, where $\alpha(CO_2{:}N_2)$ might be much lower due to less effective blocking of zeolitic pores by CO_2 at this condition.

Finally, pyrolytic carbon molecular sieve (CMS) membranes comprise another important class of porous inorganic membranes that can achieve gas separation based on differences in either size or adsorption strength of mixture components in membrane micropores [25]. Recently, very high CO_2 permeance (800–1000 Barrer) coupled with high (50–70) $\alpha(CO_2{:}N_2)$ was reported for aromatic polyimide-derived CMS membranes [26]. However, such membranes usually exhibit poor size selectivity for $CO_2{:}O_2$ (<10), whereas the aminosilicate membranes developed in this study are expected to offer $CO_2{:}O_2$ selectivities close to those of $CO_2{:}N_2$ (based on measurements with Ar).

4. Conclusions

An extensive experimental investigation has been carried out in order to prepare novel aminosilicate membranes for enhanced CO_2/air separation, and characterize their separation property at 22 °C for gas feeds of 1–20 vol.% CO_2-balance N_2, and RH of 0–40%. The new membranes appear to separate CO_2 from N_2 based on a combination of molecular sieving (e.g. size effects) and preferential CO_2 adsorption/pore blocking mechanism, and the obtained $CO_2{:}N_2$ separation factors appear to be the highest among values reported for other microporous inorganic membranes such as zeolite, sol–gel silica or pyrolytic carbon. The major results of this study can be summarized as follows:

- The synthesis of such membranes is rather challenging, especially at relatively high amine loading, e.g. ratio of $-NH_2{:}Si \geq 0.5$, since the basic character of $-NH_2$ groups raises compatibility issues with the standard polymeric sol–gel route for synthesis of molecular sieving silica membranes under acidic conditions.
- Pore size control is essential for improving the CO_2 selectivity of these membranes. The single-component gas permeation results suggest that the pore size of the silica membranes with incorporated amine is larger than standard, pure silica membranes, probably because of less efficient interpenetration of the silica clusters contained in the precursor silica sol used for membrane deposition. However, prolonged aging of the membranes results in considerable increase of the $\alpha(CO_2{:}N_2)$, at the expense of CO_2 permeance, which suggests that the pore size and porosity of the membrane is decreasing as a result of densification of the inorganic silica framework.
- Efficient removal of HCl bound on the $-NH_2$ groups is essential for ensuring strong $-NH_2{:}CO_2$ interactions during gas permeation, and this can be achieved by a mild but prolonged treatment involving permeation of H_2O vapor under an external partial pressure gradient imposed across the membrane. On the other hand, treatments with NH_3 or ethanolamine vapors result in densification of the membrane with simultaneous loss of both permeance and selectivity.

Acknowledgements

We are grateful to NASA for financial support of this study under contract NAG9-1324. We also thank Dr. Catherine Thibaud-Erkey and Mr. Tim A. Nalette of Hamilton Sundstrand Space System International for technical discussions. Sandia is a multiprogram laboratory operated by Sandia Corporation, a Lockheed Martin Company, for the United States Department of Energy's National Nuclear Security Administration under Contract DE-AC04-94AL85000.

References

[1] R.W. Baker, Ind. Eng. Chem. Res. 41 (2002) 1393–1411.
[2] K. Kusakabe, T. Kuroda, S. Morooka, J. Membr. Sci. 148 (1998) 13–23.

[3] M.G. Sedigh, L. Xu, T.T. Tsotsis, M. Sahimi, Ind. Eng. Chem. Res. 38 (1999) 3367–3380.
[4] R.M. de Vos, H. Verweij, J. Membr. Sci. 143 (1998) 37–51.
[5] C.-Y. Tsai, S.-Y. Tam, Y. Lu, C.J. Brinker, J. Membr. Sci. 169 (2000) 255–268.
[6] H. Chen, A.S. Kovvali, S. Majumdar, K.K. Sircar, Ind. Eng. Chem. Res. 38 (1999) 3489–3498.
[7] H. Chen, A.S. Kovvali, K.K. Sircar, Ind. Eng. Chem. Res. 39 (2000) 2447–2458.
[8] A.S. Kovvali, K.K. Sircar, Ind. Eng. Chem. Res. 40 (2001) 2502–2511.
[9] A.S. Kovvali, K.K. Sircar, Ind. Eng. Chem. Res. 41 (2002) 2287–2295.
[10] C.-Y. Tsai, I. Guray, X. Tang, T.A. Nalette, C. Thibaud-Erkey, C.J. Brinker, G. Xomeritakis, Novel amine-functional membrane for metabolic CO_2 removal from spacesuit breathing loop, American Institute of Physics Proceedings: Space Technology & Applications International Forum, 654, 2003, pp. 861–868.
[11] Y. Lu, G. Cao, R.P. Kale, S. Prabakar, G.P. López, C.J. Brinker, Chem. Mater. 11 (1999) 1223–1229.
[12] G. Xomeritakis, S. Naik, C.M. Braunbarth, C.J. Cornelius, R. Pardey, C.J. Brinker, J. Membr. Sci. 215 (2003) 225–233.
[13] G. Xomeritakis, S. Nair, M. Tsapatsis, Microp. Mesop. Mater. 38 (2000) 61–73.
[14] V. Nikolakis, G. Xomeritakis, A. Abibi, M. Dickson, M. Tsapatsis, D.G. Vlachos, J. Membr. Sci. 184 (2001) 209–219.
[15] S. Kim, J. Ida, V.V. Guliants, Y.S. Lin, Ordered mesostructured silica membranes for carbon dioxide separation from flue gas, in: Proceeding of the AIChE Annual Meeting, paper #72b, San Francisco, CA, 16–21 November, 2003.
[16] R. Bredesen, K. Jordal, O. Bolland, Chem. Eng. Process. 43 (2004) 1129–1158.
[17] H. Fan, Y. Lu, A. Stump, S.T. Reed, T. Baer, R. Schunk, V. Perez-Luna, G.P. López, C.J. Brinker, Nature 405 (2000) 56–60.
[18] N. Liu, R.A. Assink, B. Smarsly, C.J. Brinker, Chem. Commun. (2003) 1146–1147.
[19] C.J. Brinker, R. Sehgal, S.L. Hietala, R. Deshpande, D.M. Smith, D. Loy, C.S. Ashley, J. Membr. Sci. 94 (1994) 85–102.
[20] H.Y. Huang, R.T. Yang, D. Chinn, C.L. Munson, Ind. Eng. Chem. Res. 42 (2003) 2427–2433.
[21] R.M. de Vos, W.F. Maier, H. Verweij, J. Membr. Sci. 158 (1999) 277–288.
[22] K. Kusakabe, T. Kuroda, A. Murata, S. Morooka, Ind. Eng. Chem. Res. 36 (1997) 649–655.
[23] K. Kusakabe, T. Kuroda, K. Uchino, Y. Hasegawa, S. Morooka, AIChE J. 45 (1999) 1220–1226.
[24] Y. Hasegawa, K. Watanabe, K. Kusakabe, S. Morooka, Sep. Purif. Technol. 22–23 (2001) 319–325.
[25] A.B. Fuertes, Adsorption 7 (2001) 117–129.
[26] H.B. Park, Y.K. Kim, J.M. Lee, S.Y. Lee, Y.M. Lee, J. Membr. Sci. 229 (2004) 117–127.